Molecular Therapy
Original Article

Improved Intravitreal AAV-Mediated Inner Retinal Gene Transduction after Surgical Internal Limiting Membrane Peeling in Cynomolgus Monkeys

Kazuhisa Takahashi,[1,2] Tsutomu Igarashi,[1,2] Koichi Miyake,[1] Maika Kobayashi,[2] Chiemi Yaguchi,[2] Osamu Iijima,[1] Yoshiyuki Yamazaki,[1] Yuko Katakai,[3] Noriko Miyake,[1] Shuhei Kameya,[4] Takashi Shimada,[1] Hiroshi Takahashi,[2] and Takashi Okada[1]

[1]Department of Biochemistry and Molecular Biology, Nippon Medical School, Tokyo 113-8602 Japan; [2]Department of Ophthalmology, Nippon Medical School, Tokyo 113-8602, Japan; [3]The Corporation for Production and Research of Laboratory Primates, Ibaraki 305-0843, Japan; [4]Department of Ophthalmology, Nippon Medical School, Chiba Hokusoh Hospital, Chiba 270-1694, Japan

The retina is an ideal target for gene therapy because of its easy accessibility and limited immunological response. We previously reported that intravitreally injected adeno-associated virus (AAV) vector transduced the inner retina with high efficiency in a rodent model. In large animals, however, the efficiency of retinal transduction was low, because the vitreous and internal limiting membrane (ILM) acted as barriers to transduction. To overcome these barriers in cynomolgus monkeys, we performed vitrectomy (VIT) and ILM peeling before AAV vector injection. Following intravitreal injection of 50 μL triple-mutated self-complementary AAV serotype 2 vector encoding EGFP, transduction efficiency was analyzed. Little expression of GFP was detected in the control and VIT groups, but in the VIT+ILM group, strong GFP expression was detected within the peeled ILM area. To detect potential adverse effects, we monitored the retinas using color fundus photography, optical coherence tomography, and electroretinography. No serious side effects associated with the pretreatment were observed. These results indicate that surgical ILM peeling before AAV vector administration would be safe and useful for efficient transduction of the nonhuman primate retina and provide therapeutic benefits for the treatment of retinal diseases.

INTRODUCTION

The retina is an ideal target for gene therapy because of its easy accessibility and limited immunological response, as well as its availability for noninvasive functional and structural examination.[1] Several clinical trials of gene therapies for the treatment of Leber congenital amaurosis,[2–5] choroideremia,[6] and age-related macular degeneration[7] have recently been conducted. In all of those trials, an adeno-associated virus (AAV) vector was used for gene transfer because of its lack of pathogenicity, broad range of host and cell-type tropism, and ability to transduce both dividing and nondividing cells. In these clinical studies, subretinal injection was typically used to administer the AAV vector to the retina. However, subretinal injection induces an iatrogenic retinal detachment by making a space between the outer nuclear layer and the retinal pigment epithelium (RPE). Moreover, several adverse effects, including foveal thinning, macular holes, choroidal effusion, and ocular hypo- or hypertension have been observed during the immediate postoperative days.[2,3,8,9] Consequently, subretinal injection can potentially lead to permanent visual dysfunction.[10]

Another approach to administering an AAV vector into the retina is intravitreal injection, which has also been used in clinical trials. We previously reported that in a rodent model, an intravitreally administered AAV vector transduced the inner retina without adverse effects, whereas a subretinally administered vector transduced photoreceptor cells and the RPE, but decreased electroretinography (ERG) amplitudes.[11] Because our ultimate goal is to develop a gene therapy for inner retinal disease such as glaucoma, intravitreal injection would seem to be a more suitable method for efficient transduction into the inner retina than subretinal injections, and it is less invasive and does not induce retinal detachment.[10]

Because macaque monkeys closely match humans phylogenetically, as well as with respect to the structural features of their eyes, there has been great interest in determining the efficiency and pattern of retinal transduction in nonhuman primates, as well as the efficacy of expressed therapeutic proteins before clinical trials in humans. Although retinal transduction through intravitreal AAV administration has been reported for the primate retina, the transduction efficiency was lower than into the mouse retina.[12] It was reported that the vitreous and internal limiting membrane (ILM) form a barrier to transduction.[13] We hypothesized that simply removing that barrier prior to vector injection would improve the efficiency of transduction into the inner retina. Therefore, the aim of this study was to

Received 9 May 2016; accepted 6 October 2016;
http://dx.doi.org/10.1016/j.ymthe.2016.10.008.

Correspondence: Koichi Miyake, Department of Biochemistry and Molecular Biology, Nippon Medical School, Sendagi, Bunkyo-ku, Tokyo, 113-8602, Japan.
E-mail: kmiyake@nms.ac.jp

Table 1. Animal Characteristics, Surgical Treatment, and Inflammation

No	ID	Sex	BW (kg)	Age (years)	Eye	Pre-treatment	Inflammation
1	1310102013	female	2.90	13	1R	VIT	+
					1L	VIT+ILM	+
2	1310308088	female	3.56	11	2R	VIT	+
					2L	NO	+
3	1310412153	female	2.92	10	3R	VIT+ILM	–
					3L	NO	–

BW, body weight; ILM, internal limiting membrane peeling; L, left; NO, no operation; R, right; VIT, vitrectomy.

develop an effective method to efficiently transduce the inner retina through intravitreal AAV injection in a nonhuman primate. To test that idea, we performed vitrectomy (VIT) and ILM peeling in cynomolgus monkeys 1 month before AAV vector injection. After intravitreal injection of triple-mutated (Y444+500+730F) self-complementary AAV serotype 2 vector encoding EGFP (tm-scAAV2/GFP), which effectively transduced the rodent inner retina after intravitreal injection,[14] transduction efficiency and adverse effects were assessed.

RESULTS

Efficient Transduction of the Nonhuman Primate Retina after Surgical ILM Peeling

To assess the efficiency of AAV-mediated retinal transduction in cynomolgus monkeys, we divided their six eyes into three groups: two eyes received vitrectomy (VIT) 1 month before AAV injection (group VIT), two eyes received VIT and ILM peeling 1 month before AAV vector injection (group VIT+ILM), and the remaining two eyes were left untreated before AAV vector injection (control) (Figure S1; Table 1). We first analyzed GFP expression by acquiring images of fundus fluorescence in vivo using a fundus camera. However, no obvious GFP expression was detected. Therefore, 19 weeks after intravitreal injection of 50 μL tm-scAAV2/GFP vector, transduction efficiency was assessed immunohistochemically using an anti-GFP antibody. Because the RPE can show autofluorescence in aged monkeys, we also performed a "no-secondary" control for the anti-GFP immunostaining (Figure S2A). GFP expression in the RPE was detected without a secondary antibody. Moreover, GFP expression in the RPE was observed in the eyeball without administration of tm-scAAV2/EGFP, indicating that the RPE exhibits autofluorescence (Figure 1A; Figure S2, white arrows). Little expression of GFP was detected in the control group and group VIT. On the other hand, strong expression of GFP was seen in group VIT+ILM at the macula (Figure 1A, upper row) and at about 1500–2000 μm temporal from the macula (temporal fovea) (Figure 1A, lower row).

To evaluate the area of GFP expression, we analyzed images recorded in the same setting for each eye at the temporal fovea and at about 1,000–1,500 μm nasal from the macula (nasal fovea) using Photoshop and ImageJ software (see Materials and Methods for details). The GFP expression area was wider in group VIT+ILM than in the control group or group VIT (Figure 1B). We also analyzed the location of GFP expression in group VIT+ILM after staining the ILM with periodic acid-Schiff (PAS). The edge of the area where the ILM was peeled is flanked by red triangles in Figure 2A. Notably, the area of strong GFP expression (flanked by white triangles) matched the ILM-peeled area (Figure 2B). Furthermore, immunohistochemical staining using an anti-glutamine synthetase antibody revealed GFP expression to be mainly in Müller cells (Figure 2C).

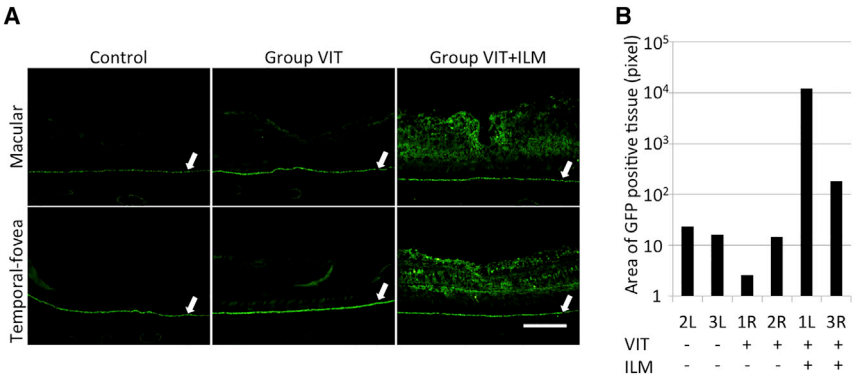

Figure 1. Histological Analysis for Detection of GFP

(A) Nineteen weeks after intravitreal injection of AAV, eyes were enucleated, sectioned, and stained for GFP. GFP expression was compared among a control group, group VIT (two eyes receiving VIT 1 month before AAV injection), and group VIT+ILM (two eyes receiving VIT and ILM peeling 1 month before AAV injection) at the macula and temporal fovea (1,500–2,000 μm temporal from the macula). White arrows indicate the RPE, which showed autofluorescence. Little GFP expression was detected in the control group or group VIT. Strong GFP expression was detected in group VIT+ILM (original magnification ×200; scale bar, 200 μm). (B) GFP expression areas (in pixels) were determined using ImageJ software and Photoshop software. The area of GFP expression in group VIT+ILM was broader than in the control group or group VIT.

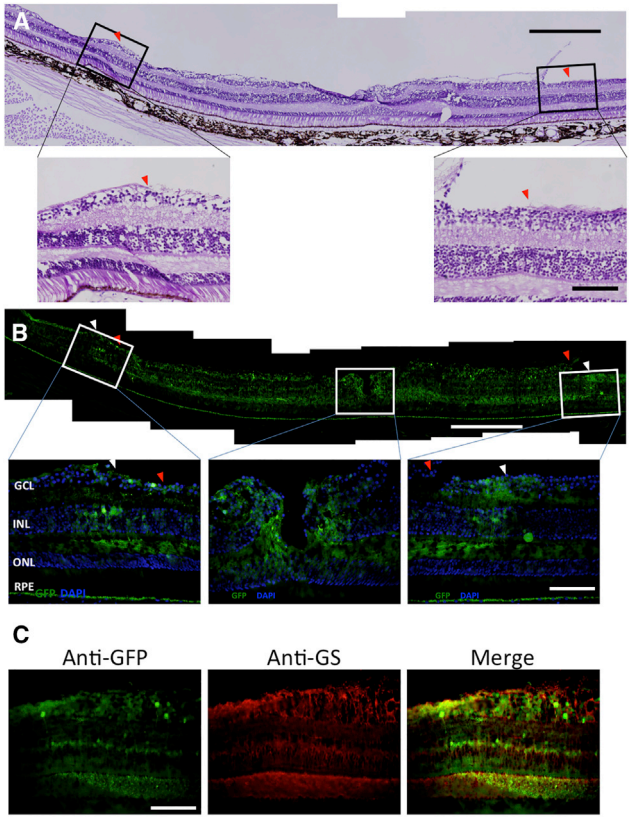

Figure 2. GFP Expression Was Limited to the ILM-Peeled Area

Histological evaluation of GFP expression in the left eye of monkey 1, belonging to group VIT+ILM. (A) Periodic acid-Schiff staining (scale bar, 500 μm) and magnified images (original magnification ×400; scale bar, 100 μm). Red triangles indicate the boundaries of the ILM peeling. (B) Anti-GFP staining (scale bar, 500 μm). White triangles indicate the boundaries between strong and weak GFP expression areas. The location of strong GFP expression (flanked by white triangles) nearly matches the area of ILM peeling (flanked by red triangles). Magnified images of anti-GFP staining at the temporal fovea (left), macula (middle), and nasal fovea (1,000–1,500 μm nasal from the macula) (right) are shown. Original magnification ×400; scale bar, 100 μm. Nuclei were stained with DAPI. (C) Specific staining for Müller cells using an anti-glutamine synthetase (GS) antibody in the temporal fovea in group VIT+ILM (left). Anti-GFP staining is also shown (middle). The figures were merged using ImageJ software (right). GCL, ganglion cell layer; INL, inner nuclear layer; ONL, outer nuclear layer; RPE, retinal pigment epithelium.

No Retinal Damage on Optical Coherence Tomography after AAV Injection

To assess retinal damage, including retinal edema, after AAV injection, we performed optical coherence tomography (OCT) to examine the retinal structure and thickness. In all groups, no changes in retinal structure were observed during the experimental period (Figure 3A). In addition, when we measured retinal thickness at the macula and para-fovea (1,000 μm from the macula) on OCT images, we found that retinal thickness had not changed over the course of the experimental period (Figure 3B).

Color Fundus Photography Revealed No Abnormal Findings except Transient Intraocular Inflammation

We also examined images of the fundus to evaluate adverse events associated with the AAV injection. No abnormal findings were observed in fundus photographs taken between a time just prior to AAV vector injection (pre-AAV) and just prior to euthanasia (pre-euthanasia) in any groups (Figure 4A). However, the fundus photographs did reveal intraocular inflammation in both eyes of monkey 1 during weeks 2–6 after AAV injection and in both eyes of monkey 2 during weeks 3–6 after AAV injection (Figure S3; Table 1). No inflammation was detected in both eyes of monkey 3. By 8 weeks after AAV injection, the inflammation detected in monkeys 1 and 2 had disappeared without local or systemic administration of a steroid. Fluorescein angiography confirmed the absence of inflammation 13 weeks after AAV injection (Figure 4B).

Transient Reduction of a- and b-Waves on ERG

Finally, we used ERG to estimate retinal function. The graphs in Figure 5 were plotted using the averaged data from the two eyes in each group. The b-wave of dark-adapted 0.01 full-field ERGs was mildly reduced 2 weeks after AAV injection, but the amplitude had returned to baseline (pre-AAV) 2 months after AAV injection (Figure 5A). Similar transient reductions in the b-wave seen in dark-adapted 0.01 full-field ERGs were observed in all groups. In group VIT, the amplitudes of the a- and b-waves on dark-adapted 3.0 and light-adapted 3.0 full-field ERGs were mildly reduced 1 month after AAV injection, but the amplitudes had returned to baseline 2 months after AAV injection (Figures 5B–5E).

DISCUSSION

In this report, we showed that surgical ILM peeling improves the efficiency of tm-scAAV2/GFP vector transduction of Müller cells after intravitreal injection. Furthermore, we detected more efficient transduction in areas with ILM peeling than in areas with intact ILM. These findings could be helpful for targeted transduction using an AAV vector.

Petrs-Silva et al.[14] showed that tm-scAAV2/GFP vector efficiently transduced the rodent inner retina after intravitreal administration. In nonhuman primates, by contrast, the area of transduction after intravitreal administration of AAV2 was confined to a narrow area surrounding the macula,[12] indicating that physical barriers such as the nerve fiber layer (NFL) or ILM limit retinal transduction. To overcome this barrier, we performed VIT and ILM peeling 1 month before AAV injection, which enabled us to efficiently transduce the retinas of cynomolgus monkeys.

Dalkara et al.[13] reported that digesting the ILM using a nonspecific protease improved the efficiency of AAV-mediated transduction in nonhuman primates. We achieved efficient transduction through surgical ILM peeling. Detection of Müller cell fragments following ILM peeling suggests the procedure causes injury to Müller cells.[15] Previous studies reported that this injury leads to dissociated optic nerve fiber layer appearance and retinal dimpling, as well as changes in

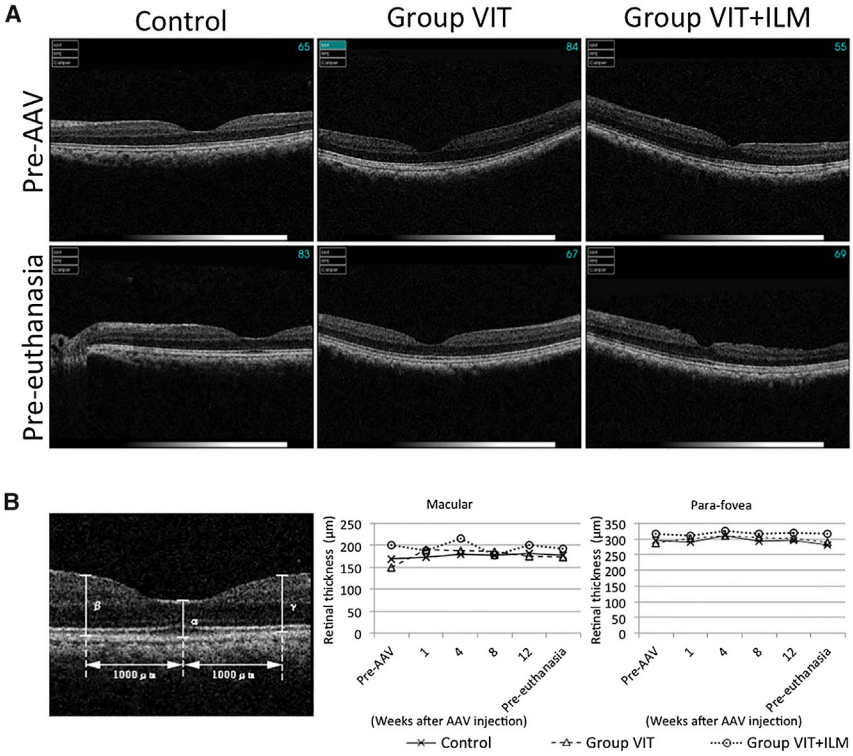

Figure 3. Comparison of Retinal Thickness throughout the Experimental Period Recorded Using Optical Coherence Tomography

The OCT recorded at just prior to AAV vector injection (Pre-AAV); 1, 4, 8, and 12 weeks after AAV vector injection; and just prior to euthanasia (Pre-euthanasia). (A) OCT images recorded pre-AAV (upper row) and pre-euthanasia (lower row). (B) Retinal thickness was measured at the macula (α) and two para-foveal points (β, γ; 1,000 μm from the macular). Data from the two eyes in each group were averaged and plotted.

the focal macular ERG, but no abnormalities in visual acuity or field were detected.[16–18] Furthermore, because surgical ILM peeling is commonly performed in clinical ophthalmology to treat macular holes and other ailments,[19] surgical peeling may be a safer way to remove the ILM than use of a nonspecific protease.

Intraocular inflammation was observed in four of six eyes (Table 1). We do not think the inflammation was related to the surgery because it was not observed during the first month after surgery. Moreover, the inflammation began only about 2 weeks after AAV injection, suggesting the inflammation may be associated with the AAV administration. Consistent with that idea, AAV-mediated transduction of the retina in humans, monkeys, and dogs reportedly causes transient inflammation that does not adversely affect visual function.[3,20] In addition, we detected no morphological changes on color fundus images or OCT between the pre-AAV and pre-euthanasia injections (23 weeks after operation). However, Pichi et al.[21] observed lower retinal nerve fiber layer thickness 6 months post-operatively, suggesting longer post-operative observation may be needed.

We evaluated retinal function using full-field ERGs. The amplitude of the b-wave on dark-adapted 0.01 full-field ERGs tended to be decreased 2 weeks after AAV vector injection, but returned to baseline within 2 months after vector injection. Because similar decreases were observed in all groups, including the control group, it does not appear that the VIT or ILM peeling caused the change in ERG amplitude. The amplitudes of the a- and b-waves on dark-adapted 3.0 and light-adapted 3.0 full-field ERGs in group VIT were mildly reduced 1 month after AAV injection. Given that group VIT+ILM received more invasive pretreatment than group VIT, group VIT+ILM was expected to exhibit greater reductions of ERG amplitude than group VIT. However, similar a- and b-wave reductions were not observed in dark-adapted 3.0 and light-adapted 3.0 full-field ERGs with group VIT+ILM, which suggests that the reductions were not the result of the pretreatment. In addition, when we compared the ERGs between the groups with and without inflammation, we found that the b-wave amplitude on dark-adapted 0.01 full-field ERG was decreased 2 weeks after AAV injection in both groups. But 3 weeks after AAV injection, the b-wave amplitude was improved in the group without inflammation, whereas it was worse in the group with inflammation (Figure S4A). It was not until 8 weeks after AAV injection that b-wave amplitudes on dark-adapted 0.01 full-field ERG returned to baseline in the group with inflammation, which coincided with improvement of the inflammation. Furthermore, the a- and b-wave amplitudes on dark-adapted 3.0 and light-adapted 3.0 full-field ERGs were reduced only in the group with inflammation during the period that the inflammation occurred (i.e., 2–6 weeks after AAV injection). The a- and b-wave amplitudes returned to baseline within 8 weeks, again coinciding with the disappearance of inflammation from color fundus images (Figures S4B–S4E). These results suggest that transient intraocular inflammation may transiently reduce ERG amplitude.

Vandenberghe et al.[22] reported that subretinal injection of 1×10^{10} vector genome (v.g.) AAV2-GFP resulted in transduction of about 30% of the RPE and photoreceptor. By comparison, the transduction levels achieved in the present study might seem lower than expected for the dose of AAV vector used. However, these results cannot be directly compared because the route of administration, promoter used to express GFP, and the AAV vector capsid all differed between the two studies. Nonetheless, possible explanations for the different transduction levels include the following: (1) because the volume of

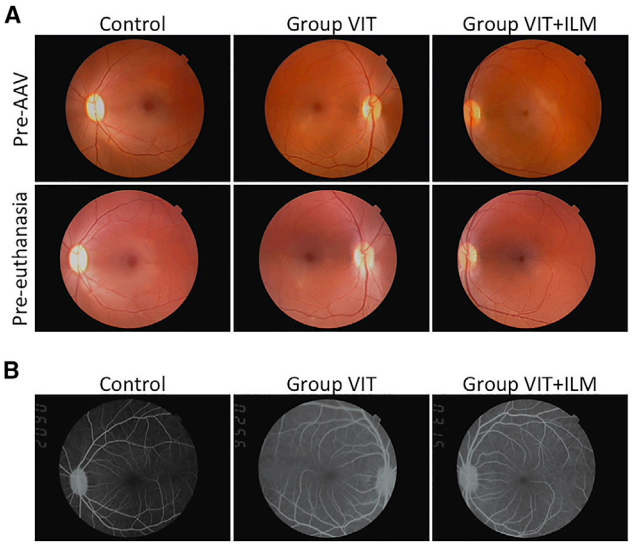

Figure 4. Color Fundus Images and Fluorescein Angiography Images
(A) Color fundus images of the left eye of monkey 3 (control) and the right and left eyes of monkey 1 (group VIT and group VIT+ILM, respectively). Images were obtained pre-AAV (upper row) and pre-euthanasia (lower row). (B) Fluorescein angiography images of the same three eyes obtained 13 weeks after AAV vector injection.

the vitreous cavity is much larger than that of the subretinal space, the administered AAV vector may have been diluted; (2) AAV capsids may have been lost because of vitritis; and (3) the efficiency of transduction into the cynomolgus monkey retina of the tm-scAAV2 vector may be low. That said, although the expression of GFP was lower in the present study than in the earlier report, it is clear that ILM peeling improved the efficiency of transduction.

In summary, we observed that AAV-mediated transduction of the nonhuman primate retina was dramatically improved by VIT and ILM peeling 1 month before AAV vector injection, without serious adverse effects. This indicates that surgical ILM peeling before AAV administration would be safe and useful for efficient transduction of the nonhuman primate retina. This method enables the AAV vector to transduce the inner macula and provide therapeutic benefits for the treatment of various diseases causing retinal dysfunction, such as glaucoma.

MATERIALS AND METHODS

Animals

Three adult female cynomolgus monkeys from the Tsukuba Primate Research Center were used for this study. Each animal weighed approximately 3 kg and was 10–13 years old (Table 1). Before any experiments, each eye was examined using fundus photos, OCT, and ERG, and no abnormalities were found. All animal procedures were conducted according to the Association for Research in Vision and Ophthalmology (ARVO) statement for the Use of Animals in Ophthalmic and Vision Research and the Animal Experimental Ethical Review Committee of Nippon Medical School.

Production and Purification of AAV Vector

An AAV packaging plasmid (pACG2-3M) generated by introducing a triple tyrosine-to-phenylalanine (Y444+500+730F) mutation into the virion protein 3 (VP3) region of the AAV serotype 2 capsid and a self-complementary AAV vector plasmid carrying cDNA encoding EGFP (pdsCBA-GFP) were kindly provided by Dr. Srivastava.[27] A recombinant scAAV vector (tm-scAAV2/GFP) was produced by transient triple transfection of HEK293 cells as previously described.[11,23] The AAV vector particles were harvested from the transfected cells using an AAVpro Purification Kit (AAV2) (TakaRa Bio) according to the manufacturer's instructions. Thereafter, the buffer containing the AAV vector was changed to PBS (−) using an Amicon Ultra-15 Centrifugal Filter Unit (molecular weight cutoff, 30 kDa) (Merck Millipore), which was centrifuged for 5 min at 5,000 × *g*. The particle titers of the AAV vector were determined by qPCR analysis using a 7500 Fast Real-Time PCR Instrument (Applied Biosystems). The total vector genome (v.g.) number for tm-scAAV2/EGFP was 1.9×10^{13} v.g./mL.

Surgical Procedures

All animals were anesthetized using mixed anesthesia composed of ketamine and xylazine. Among the six eyes in the three monkeys, two eyes received standard three-port VIT before AAV injection. For this procedure, three ports (25G) were made, after which 200–400 μl triamcinolone suspension (MaQaid; Wakamoto) was injected into the vitreous cavity to enable visualization of the cortical vitreous. The cortical vitreous was then removed. Two eyes received ILM peeling in addition to the standard three-port VIT (Figure S1; Table 1). The ILM was visualized using 200–400 μl Brilliant Blue G (Sigma-Aldrich)[24] and peeled using a Diamond Dusted Sweeper (Dutch Ophthalmic Research Center [International]) and ILM forceps (Alcon Japan). The remaining two received no pretreatment. The VIT and ILM peeling were performed by using a Stellaris PC (Bausch & Lomb) under an operating microscope (OPMI MDO; Carl Zeiss).

Intravitreal injection

All six eyes were injected with AAV 1 month after pretreatment. We chose 1 month for the time to avoid the influence of any adverse effect of pretreatment. All animals were anesthetized using mixed anesthesia (ketamine and xylazine), after which a 30G needle was penetrated into the vitreous at the pars plana,[25] and 50 μL tm-scAAV2/GFP was administered.

Optical Coherence Tomography

OCT was performed to evaluate the thickness of the macula and parafovea using a 3D OCT-1000 mark II (Topcon). After animals were anesthetized with mixed anesthesia (ketamine and xylazine), OCTs were taken just prior to the operation; prior to AAV injection; 1, 4, 8, and 12 weeks after AAV injection; and prior to euthanasia. Retinal thickness was estimated in two places: just below and an average of 1,000 μm nasal and temporal from the macula.

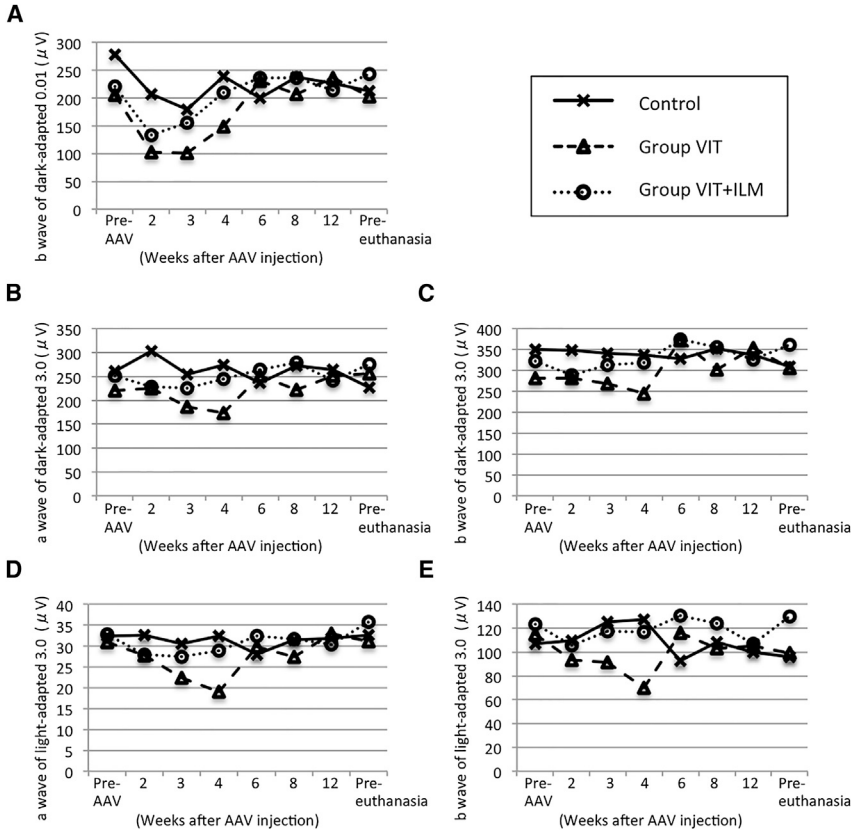

Figure 5. Amplitudes of a- and b-Waves in Full-Field ERGs

Full-field ERGs were recorded using the standard International Society for Clinical Electrophysiology of Vision (ISCEV) time course just prior to AAV vector injection (pre-AAV); 2, 3, 4, 6, 8, and 12 weeks after AAV vector injection; and just prior to euthanasia (pre-euthanasia). The ERG amplitudes in the two eyes from each group were averaged and plotted. (A) Amplitudes of b-waves in dark-adapted 0.01 full-field ERGs. (B and C) Amplitudes of a-waves (B) and b-waves (C) in dark-adapted 3.0 full-field ERGs. (D and E) Amplitudes of a-waves (D) and b-waves (E) in light-adapted 3.0 full-field ERGs.

Fundus Color Photography, Fundus Images of GFP Fluorescence, and Fluorescein Angiography

After animals were anesthetized with mixed anesthesia (ketamine and xylazine), color fundus photographs and fundus images of GFP fluorescence and fluorescein angiographs were taken using a fundus camera (model TRC-NW6SF; Topcon). Color fundus photographs and fundus images of GFP fluorescence were taken prior to AAV vector injection; 1, 2, 3, 4, 6, 8, and 12 weeks after AAV vector injection; and prior to euthanasia. Fluorescein angiographs were taken using fluorescein (Alcon Japan) 13 weeks after AAV injection.

Electroretinography

After animals were anesthetized using mixed anesthesia (ketamine and xylazine), full-field ERGs were taken for assessment of retinal function. Full-field ERGs were recorded according to the International Society for Clinical Electrophysiology of Vision (ISCEV) standard[26] prior to AAV vector injection; 2, 3, 4, 6, 8, and 12 weeks after AAV vector injection; and prior to euthanasia. Recordings were made using a synchronized trigger and summing amplifier (Primus; Mayo) with a stimulation device (LS-W; Mayo). The amplitudes recorded from the two eyes in each group were averaged and plotted.

Histological Analysis

Animals were euthanatized 19 weeks after AAV vector injection for histological analysis. The eyes were enucleated and fixed with 4% paraformaldehyde in PBS overnight at 4°C. The cornea and lens were then removed and again fixed in 4% paraformaldehyde in PBS overnight at 4°C. The eyes were then sequentially soaked in 10% sucrose for 4 hr, 20% sucrose overnight, and 30% sucrose overnight, after which they were frozen in O.C.T. compound (Tissue-Tek; Sakura Finetechnical) on dry ice ethanol, and 10-μm-thick sections were cut using a CM1950 cryostat (Leica Microsystems). PAS staining was performed to detect the area of peeled ILM.

Immunohistochemistry

After blocking thin sections (10 μm) in 10% goat serum in PBS containing 0.05% Triton X (PBST), the sections were incubated for 2 hr at room temperature with a rabbit anti-GFP IgG antibody (1:1,000 dilution; Invitrogen). The sections were then washed three times with PBST and incubated with Alexa 488 goat anti-rabbit IgG (1:500 dilution; Invitrogen) for 2 hr at room temperature. To detect Müller cells, the sections were immune activated with HistVT One (Nacalai Tesque) and incubated overnight at 4°C with a mouse anti-glutamine synthetase IgG (1:500 dilution; Millipore). Then after being washed three times with PBST, the sections were incubated with Alexa 594-conjugated donkey anti-mouse IgG (1:500 dilution; Invitrogen) for 2 hr at room temperature. The stained sections were washed with PBST, mounted using a medium containing DAPI (Vector Laboratories), and examined under a fluorescence microscope (DP-70; Olympus Fluorescence Microscope). To analyze GFP expression in each eye, we examined seven slides containing sections 50 μm apart at the middle of the macula center. Two images of corresponding regions were taken from each slide using the same camera gain and time settings (×200, 0.25 s). To compare GFP expression, we analyzed each image pixel using ImageJ (Version 1.49v; NIH) and Photoshop (Adobe Systems) software.

SUPPLEMENTAL INFORMATION

Supplemental Information includes four figures and can be found with this article online at http://dx.doi.org/10.1016/j.ymthe.2016.10.008.

AUTHOR CONTRIBUTIONS

K.T. performed most of the experiments, wrote the manuscript, and contributed to the study concept and design. T.I. designed the experiments, performed animal experiments, conducted the experiments, and wrote the paper. K.M. conducted the experiments and wrote the paper. M.K., Y.Y., and Y.K. performed animal experiments. C.Y., N.M., and S.K. interpreted the data and supervised the project. O.I. produced and purified AAV vector. H.T. conducted the experiments and performed animal experiments. T.S. and T.O. conducted the experiments. All authors read and approved the manuscript.

CONFLICTS OF INTEREST

The authors have no conflicts of interest to declare.

ACKNOWLEDGMENTS

We thank Dr. Arun Srivastava at the University of Florida for providing the pACG2-3M (pAAV2-Y730+500+444F) packaging plasmids and pdsCBA-GFP vector plasmid. We also thank Dr. Atsushi Mizota at the University of Teikyo for instruction on the ERG method in monkeys. This study was conducted through the Cooperative Research Program in the Tsukuba Primate Research Center, National Institutes of Biomedical Innovation, Health and Nutrition. The eyeball without administration of tm-scAAV2/EGFP was provided by the Non-human Primate Reagent and Resource Program in Tsukuba Primate Research Center, National Institute of Biomedical Innovation, Health and Nutrition.

REFERENCES

1. Bennett, J., Chung, D.C., and Maguire, A. (2012). Gene delivery to the retina: from mouse to man. Methods Enzymol. *507*, 255–274.
2. Maguire, A.M., Simonelli, F., Pierce, E.A., Pugh, E.N., Jr., Mingozzi, F., Bennicelli, J., Banfi, S., Marshall, K.A., Testa, F., Surace, E.M., et al. (2008). Safety and efficacy of gene transfer for Leber's congenital amaurosis. N. Engl. J. Med. *358*, 2240–2248.
3. Bainbridge, J.W., Mehat, M.S., Sundaram, V., Robbie, S.J., Barker, S.E., Ripamonti, C., Georgiadis, A., Mowat, F.M., Beattie, S.G., Gardner, P.J., et al. (2015). Long-term effect of gene therapy on Leber's congenital amaurosis. N. Engl. J. Med. *372*, 1887–1897.
4. Cideciyan, A.V., Aleman, T.S., Boye, S.L., Schwartz, S.B., Kaushal, S., Roman, A.J., Pang, J.J., Sumaroka, A., Windsor, E.A., Wilson, J.M., et al. (2008). Human gene therapy for RPE65 isomerase deficiency activates the retinoid cycle of vision but with slow rod kinetics. Proc. Natl. Acad. Sci. USA *105*, 15112–15117.
5. Maguire, A.M., High, K.A., Auricchio, A., Wright, J.F., Pierce, E.A., Testa, F., Mingozzi, F., Bennicelli, J.L., Ying, G.S., Rossi, S., et al. (2009). Age-dependent effects of RPE65 gene therapy for Leber's congenital amaurosis: a phase 1 dose-escalation trial. Lancet *374*, 1597–1605.
6. MacLaren, R.E., Groppe, M., Barnard, A.R., Cottriall, C.L., Tolmachova, T., Seymour, L., Clark, K.R., During, M.J., Cremers, F.P., Black, G.C., et al. (2014). Retinal gene therapy in patients with choroideremia: initial findings from a phase 1/2 clinical trial. Lancet *383*, 1129–1137.
7. Rakoczy, E.P., Lai, C.-M., Magno, A.L., Wikstrom, M.E., French, M.A., Pierce, C.M., Schwartz, S.D., Blumenkranz, M.S., Chalberg, T.W., Degli-Esposti, M.A., and Constable, I.J. (2015). Gene therapy with recombinant adeno-associated vectors for neovascular age-related macular degeneration: 1 year follow-up of a phase 1 randomised clinical trial. Lancet *386*, 2395–2403.
8. Jacobson, S.G., Cideciyan, A.V., Ratnakaram, R., Heon, E., Schwartz, S.B., Roman, A.J., Peden, M.C., Aleman, T.S., Boye, S.L., Sumaroka, A., et al. (2012). Gene therapy for leber congenital amaurosis caused by RPE65 mutations: safety and efficacy in 15 children and adults followed up to 3 years. Arch. Ophthalmol. *130*, 9–24.
9. Vandenberghe, L.H., Bell, P., Maguire, A.M., Xiao, R., Hopkins, T.B., Grant, R., Bennett, J., and Wilson, J.M. (2013). AAV9 targets cone photoreceptors in the nonhuman primate retina. PLoS ONE *8*, e53463.
10. Carvalho, L.S., and Vandenberghe, L.H. (2015). Promising and delivering gene therapies for vision loss. Vision Res. *111* (Pt B), 124–133.
11. Igarashi, T., Miyake, K., Asakawa, N., Miyake, N., Shimada, T., and Takahashi, H. (2013). Direct comparison of administration routes for AAV8-mediated ocular gene therapy. Curr. Eye Res. *38*, 569–577.
12. Yin, L., Greenberg, K., Hunter, J.J., Dalkara, D., Kolstad, K.D., Masella, B.D., Wolfe, R., Visel, M., Stone, D., Libby, R.T., et al. (2011). Intravitreal injection of AAV2 transduces macaque inner retina. Invest. Ophthalmol. Vis. Sci. *52*, 2775–2783.
13. Dalkara, D., Kolstad, K.D., Caporale, N., Visel, M., Klimczak, R.R., Schaffer, D.V., and Flannery, J.G. (2009). Inner limiting membrane barriers to AAV-mediated retinal transduction from the vitreous. Mol. Ther. *17*, 2096–2102.
14. Petrs-Silva, H., Dinculescu, A., Li, Q., Deng, W.T., Pang, J.J., Min, S.H., Chiodo, V., Neeley, A.W., Govindasamy, L., Bennett, A., et al. (2011). Novel properties of tyrosine-mutant AAV2 vectors in the mouse retina. Mol. Ther. *19*, 293–301.
15. Nakamura, T., Murata, T., Hisatomi, T., Enaida, H., Sassa, Y., Ueno, A., Sakamoto, T., and Ishibashi, T. (2003). Ultrastructure of the vitreoretinal interface following the removal of the internal limiting membrane using indocyanine green. Curr. Eye Res. *27*, 395–399.
16. Ito, Y., Terasaki, H., Takahashi, A., Yamakoshi, T., Kondo, M., and Nakamura, M. (2005). Dissociated optic nerve fiber layer appearance after internal limiting membrane peeling for idiopathic macular holes. Ophthalmology *112*, 1415–1420.
17. Spaide, R.F. (2012). "Dissociated optic nerve fiber layer appearance" after internal limiting membrane removal is inner retinal dimpling. Retina *32*, 1719–1726.
18. Terasaki, H., Miyake, Y., Niwa, T., Ito, Y., Suzuki, T., Kikuchi, M., and Kondo, M. (2002). Focal macular electroretinograms before and after removal of choroidal neovascular lesions. Invest. Ophthalmol. Vis. Sci. *43*, 1540–1545.
19. Kadonosono, K., Itoh, N., Uchio, E., Nakamura, S., and Ohno, S. (2000). Staining of internal limiting membrane in macular hole surgery. Arch. Ophthalmol. *118*, 1116–1118.
20. Narfström, K., Katz, M.L., Bragadottir, R., Seeliger, M., Boulanger, A., Redmond, T.M., Caro, L., Lai, C.M., and Rakoczy, P.E. (2003). Functional and structural recovery of the retina after gene therapy in the RPE65 null mutation dog. Invest. Ophthalmol. Vis. Sci. *44*, 1663–1672.
21. Pichi, F., Lembo, A., Morara, M., Veronese, C., Alkabes, M., Nucci, P., and Ciardella, A.P. (2014). Early and late inner retinal changes after inner limiting membrane peeling. Int. Ophthalmol. *34*, 437–446.
22. Vandenberghe, L.H., Bell, P., Maguire, A.M., Cearley, C.N., Xiao, R., Calcedo, R., Wang, L., Castle, M.J., Maguire, A.C., Grant, R., et al. (2011). Dosage thresholds for AAV2 and AAV8 photoreceptor gene therapy in monkey. Sci. Transl. Med. *3*, 88ra54.
23. Miyake, N., Miyake, K., Asakawa, N., Yamamoto, M., and Shimada, T. (2014). Long-term correction of biochemical and neurological abnormalities in MLD mice model by neonatal systemic injection of an AAV serotype 9 vector. Gene Ther. *21*, 427–433.
24. Steel, D.H., Dinah, C., Madi, H.A., White, K., and Rees, J. (2014). The staining pattern of brilliant blue G during macular hole surgery: a clinicopathologic study. Invest. Ophthalmol. Vis. Sci. *55*, 5924–5931.
25. Lukason, M., DuFresne, E., Rubin, H., Pechan, P., Li, Q., Kim, I., Kiss, S., Flaxel, C., Collins, M., Miller, J., et al. (2011). Inhibition of choroidal neovascularization in a nonhuman primate model by intravitreal administration of an AAV2 vector expressing a novel anti-VEGF molecule. Mol. Ther. *19*, 260–265.
26. Marmor, M.F., Fulton, A.B., Holder, G.E., Miyake, Y., Brigell, M., and Bach, M.; International Society for Clinical Electrophysiology of Vision (2009). ISCEV Standard for full-field clinical electroretinography (2008 update). Doc. Ophthalmol. *118*, 69–77.
27. Li, M., Jayandharan, G.R., Li, B., Ling, C., Ma, W., Srivastava, A., and Zhong, L. (2010). High-efficiency transduction of fibroblasts and mesenchymal stem cells by tyrosine-mutant AAV2 vectors for their potential use in cellular therapy. Hum Gene Ther. *21*, 1527–1543.